International Journal of Basic and Applied Sciences, 14 (3) (2025) 446-457

International Journal of Basic and Applied Sciences

Website: www.sciencepubco.com/index.php/IJBAS
https://doi.org/10.14419/5ejenv72
Research paper

Optimizing EV Charging: An Implementation of The Modified Cuk Converter for High Power Factor and Low Ripple Performance

Pushpak B. Patel [1] *, Dr. Sanjay R. Vyas [2]

[1] Research scholar, Kadi Sarva Vishwavidyalaya University, Gandhinagar, Gujarat, India
[2] Professor, Electrical Department, LDRP Institute of Technology and Research, Kadi Sarva Vishwavidyalaya University, Gandhinagar, Gujarat, India
**Corresponding author E-mail: pbpatel2303@gmail.com*

Received: June 25, 2025, Accepted: July 26, 2025, Published: July 30, 2025

Abstract

Advancements in EV battery charging have enhanced overall performance and power quality. Power factor correction (PFC) converters, such as buck, boost, Cuk, Z-source, and Interleaved topologies, minimize ripple and enhance power factor. This study reviews recent charger designs, focusing on PFC converters and their role in reducing ripple and harmonic distortion. It also evaluates constant current (CC) and constant voltage (CV) charging methods through simulations to ensure stable and efficient charging. A 1.4 kW, Level-1 on-board charger was designed to provide 400V DC at 3.5A for a 400V battery pack. Simulations of a modified Cuk converter in CV and CC modes, with a battery, assessed voltage and current stabilization under varying input conditions (180V–280V). PF ranged from 0.87 to 0.97. Additional simulations with a lithium-ion battery analyzed ripple suppression and power factor stability. The results were compared with various past studies on different converter topologies to evaluate performance improvements. Furthermore, the modified converter's results were validated through hardware implementation. The modified Cuk converter maintained a stable 400V, 3.5A output with voltage and current ripple of 4.2% and 4.5%, respectively. The system achieves a PF of 0.983 in CC mode with less than 1% ripple, while CV mode maintains a power factor between 0.940 and 0.946 with a Li-ion battery. The modified Cuk converter outperformed currently available converters, and hardware results aligned closely with PSIM simulation data, confirming reliability and efficient operation. The proposed charger achieves high PF and low ripple, ensuring reliable battery charging.

Keywords: *CC and CV Control; EV Charging Systems; Modified Cuk Converter; PFC Converters; Ripple Reduction.*

1. Introduction

Significant advancements have been made in battery charging systems driven by a variety of innovative approaches. Patil and Agrawal (2015) have presented a single-stage charger that efficiently manages the ripple of the Direct Current (DC) supply, enhancing performance [1]. Kim, Kim, and Lee (2016) applied asynchronous control algorithms and proposed duty and frequency control methods to optimize the efficiency across a wide range of input and output voltage of an on-board charger (OBC) [2]., while Sujitha and Krithiga (2017) introduce the use of renewable energy sources for EV charging to promote sustainability [3]. Lu et al. (2017) proposed advanced control strategies to achieve high power density with variations in input and output for a battery charger [4]. Nguyen et al. (2018) introduced a multifunctional OBC that reduces the size and cost by integrating active power decoupling [5]. Kushwaha and Singh (2018) proposed a bridgeless Power Factor Correction (PFC) design that minimizes conduction losses as well as harmonic distortion [6]. Yilmaz et al. (2020) enhanced the EV range and reduced energy costs by integrating a PV system with a high-efficiency PFC converter [7]. Lai et al. (2020) introduced a PV-powered quick charger with a high-performance boost converter to reduce grid dependence and promote sustainable energy use [8]. Tiwary and Singh (2020) proposed a modified PFC rectifier with advanced control techniques to mitigate harmonics and THD, thereby improving efficiency [9]. Kushwaha and Singh (2021) improved the power quality and efficiency of a switched-inductor PFC converter and the flyback design [10]. Berliner et al. (2022) proposed novel General Operating Modes (GOMs) for lithium-ion battery charging, offering a more effective approach for modelling predictive control in real-time systems [11]. Patel et al. (2023) proposed a bidirectional PFC converter with zero-current switching to enhance the power density and reliability [12]. Sisir et al. (2023) revealed a DSP-based charger with high efficiency across various voltage levels, demonstrating significant advancement over regular methods [13]. This study collectively advanced the EV battery charger technology by introducing innovations that enhance system performance, power quality. Key contributions include improved power factor correction, reduced harmonic distortion, and advanced control algorithms, which collectively improve vehicle range, reduce energy cost, and enhance overall performance.

Various advancements have been made in PFC converters for EV charging. Kushwaha and Singh (2019) introduced a modified Luo PFC converter with a two-switch design and input-clamping diodes to enhance power quality and reduce ripple [14]. Jagdeesh and Indragandhi (2019) reviewed several efforts to assess the efficiency of DC-DC converters and the voltage and current stress on switches in electric vehicles powered by basic PV and fuel cell systems [15]. In (2020), Kushwaha and Singh proposed an interleaved Landsman converter combined with a fly-back converter designed to improve the performance and cost efficiency through current sharing and reduced ripple [16]. Dixir et al. (2020) proposed a simplified single-phase AC-DC buck-boost converter for EV charging, which is ideal for low-voltage applications such as golf carts and E-rickshaws, with experimental validation using a 1.0-kW prototype [17]. Choi et al. (2020) presented an interleaved isolated PFC converter for a three-phase system that utilizes zero-voltage and zero-current switching to achieve superior performance and reduce voltage stress [18]. Pandey and Singh (2021) presented a twin-stage PFC resonance charger for EVs, combining a reduced sensor-based bridgeless boost (BLB) converter with a full-bridge inductor-inductor capacitor (FBLLC) converter [19]. Papamanolis et al. (2021) proposed a universal PFC rectifier that supports both single-phase and three-phase EV chargers, ensuring full power delivery and adherence to EMI regulations [20]. Devia-Narvaez et al. (2021) presented the design of the control and power stages, along with the voltage and current waveforms obtained at the output of the implemented three-phase converter [21]. Kumar and Verma (2021) introduced a two-stage interleaved bridgeless PFC charger for 48V applications, achieving a maximum efficiency of 94% and low THD of the input current [22]. Dutta et al. (2022) proposed a single-phase bridgeless Cuk-derived PFC converter with reduced components and natural PFC operation [23], whereas Jain et al. (2022) presented a bidirectional five-level buck rectifier for EV charging applications, offering wide output regulation and bidirectional power flow for vehicle-to-grid systems [24]. Chaitanya and Sindhu (2022) developed a low-voltage two-stage on-board charger with 93% efficiency [25], and Tiwari et al. (2023) proposed a single-phase five-level PFC rectifier that reduced voltage stress [26]. Kumar and Verma (2023) also described a single-phase interleaved buck-boost PFC charger that eliminates the need for an input sensor and maintains high efficiency and low THD [27]. Patel and Vyas (2024) examined Cuk and modified Cuk converters, highlighting their ability to reduce ripple, improve the power factor, and lower harmonic distortion, thus offering superior stability for DC power supplies [28]. Bag et al. (2024) introduced the Landsman converter as an efficient low-power solution for charging EV batteries, demonstrating a superior performance through both simulation and experimental validation [29]. Jayalakshmi et al. (2024) presented various converter topologies, including a solid-state transformer (SST), for fast-charging applications, emphasizing bidirectional power flow and integration of vehicle-to-grid (V2G) technologies [30]. This advancement includes improved converter designs, such as the interleaved Landsman, modified Luo PFC, and bridgeless configurations, which address issues such as power quality enhancement, ripple reduction, simplified control, and cost- cost-effectiveness. These studies collectively advance the field by offering solutions that meet international power quality standards and accommodate various charging applications.

Recent research has examined interleaved, bridgeless, and dual-stage converter topologies to enhance performance and THD. Interleaved converters like the Landsman and buck-boost enhance current sharing and suppress ripple, but do not provide isolation and add complexity to control. Bridgeless designs reduce conduction loss and eliminate the need for a power factor correction circuit. Such an approach may increase design complexity and expense, particularly in EV chargers. This study's improved Cuk converter decreases ripple and increases PF with easy control. Significant advancements have been made in recent studies on battery and power-converter technologies. Chang et al. (2019) enhance a high-accuracy PSR CC and CV controlled AC-DC converter with a novel cable compensation method that avoids external capacitors, enhances reliability, and reduces costs [31]. Stübler et al. (2020) introduced a lithium-ion battery model using CC-CV and impedance spectroscopy to improve the accuracy of battery simulations [32]. Li et al. (2020) explored cooperative CC-CV charging for a supercapacitor using multi-charger systems, addressing current imbalances and enhancing system performance [33]. Liu et al. (2020) introduced an analytical model for Li-ion battery charging under a CC-CV profile, offering insights into battery degradation [34]. Nguyen et al. (2021) proposed a cost-effective single-phase on-board battery charger (OBC) for plug-in electric vehicles that integrates low-voltage battery charging with active power decoupling across three operating modes, reducing size and components while achieving effective performance, as verified by simulations and experiments [35]. De and Dey (2021) evaluated the critical transition point between CC and CV modes in Li-ion battery charging, highlighting its importance for battery safety and longevity [36]. He et al. (2023) implemented a hybrid control strategy for an inductive power transfer system, achieving high quality and improved performance in CC-CV battery charging [37]. These studies have made significant strides in advancing both battery and power converter technologies, including the development of high-accuracy AC-DC converters and enhanced battery modelling for more precise simulations. Innovations in cooperative charging methods and hybrid control strategies have further improved efficiency and system performance, contributing to better battery safety and longevity. Collectively, these advancements have pushed the boundaries of charger design by addressing key challenges such as ripple reduction, efficiency optimization, integration, and CC/CV charging, paving the way for future innovations in electric vehicle (EV) charging technology.

Despite advancements in EV battery charging, conventional PFC converters like buck-boost, SEPIC, and traditional Cuk converters struggle with high voltage ripple, increased switching losses, and limited power factor improvement. Many require additional PFC circuits, increasing system complexity and cost.

This study presents a modified Cuk converter that inherently improves power factor and reduces ripple without external PFC circuitry. The integration of a High-Frequency Transformer (HFT) enhances voltage regulation and galvanic isolation, improving safety. By operating in discontinuous conduction mode for the input inductor L_1 and continuous conduction mode for the output inductor L_o the converter minimizes conduction losses and voltage stress.

Through simulations in both CC and CV charging modes, the proposed design demonstrates stability across varying input voltages (180V–280V), outperforming traditional topologies. These innovations show the modified Cuk converter is a more efficient and cost-effective solution for EV battery charging.

2. Methodology

This paper shows an evaluation of the converter in battery charging technologies for EV through a simulation in PSIM. This simulation analyses the performance of power factor improvement using Modified Cuk Converter and Lithium-ion battery charging with low ripple, specifically focusing on the evaluation of charging control strategies in CC and CV modes. The simulation and hardware implementation enable a detailed assessment of the performance of the charger under various conditions.

2.1. Converter design

The modified Cuk converter is used for charging the lithium-ion battery for Electric vehicles. This converter simulates operation in both CC and CV modes using PSIM, providing a DC output of 400V and 3.5A. This simulation shows that the built-in AC-DC converter in this design produces low voltage and current ripple during operation, ensuring high-quality power. Because of its low DC ripple, good power quality, and versatility, the modified Cuk converter is an excellent choice for EV battery charging requirements. Table 1 summarizes the specifications of the modified Cuk converter for the Level-1 on-board charger.

Table 1: Parameter Selection for Modified Cuk Converter Charger

Specification	Value
Power Rating	1.4 kW
Charger Type	Level-1 on-board Charger
Input Voltage	230V (AC)
Input Current	16A
Output Voltage	400V (DC)
Output Current	3.5A
Switching frequency	50 kHz
Battery Pack Voltage	400V, 100Ah

Figure 1 illustrates the topology of the modified Cuk converter battery charger. This layout is intended to provide a DC voltage output with an enhanced input power factor and enhanced operation, making it suitable for applications of EV battery charging. The enhancements in this specific converter version focus on optimizing voltage regulation and power quality.

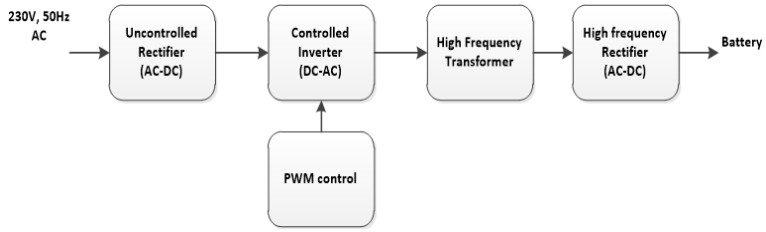

Fig. 1: Block Diagram of the Modified Cuk Converter-Based On-board EV Battery Charger with Galvanic Isolation.

The integration of a HFT into the Modified Cuk Converter opens a new level of control over voltage and ripple-something traditional Cuk or SEPIC designs don't match. Instead of depending solely on an inductor and a capacitor, the HFT introduces galvanic isolation. That means safer operation and less voltage stress on the switching devices. The converter strategically operates with DCM for the source inductor L_1 and CCM for the load side inductor L_0, achieving reduced conduction losses and stabilizing the output power. The intermediate capacitor C_1 plays a crucial role in facilitating smooth energy transfer and ensuring a consistent, sinusoidal current flow. These design enhancements contribute to better power quality, lower harmonic distortion, and improved overall performance in EV charging applications.

The modified Cuk converter operates in three main stages. Initially, a conventional bridge rectifier transforms the incoming AC voltage into DC. The second stage involves the conversion of the DC voltage into a high-frequency AC voltage. During which a HFT provides galvanic isolation between the power source and load. Finally, in the last stage, the high-frequency AC is rectified back into DC by the LC filter components. This multi-stage approach ensures a high PF and delivers a stable DC output.

When the switch is turned on, current moves from capacitor C_1 to the output through a diode and the main winding of the high-frequency transformer. As the diode enters a forward-bias state, it delivers power to inductor L_o, transferring energy from capacitor C_1 via the HFT. Simultaneously, inductor L_1 absorbs the energy.

In the second phase, when the switch is turned off, the energy stored in inductor L_1 is transferred to charge capacitor C_1 through a predetermined path that includes inductor L_1, capacitor C_1, and the diode. In this process, a freewheeling diode in the second part of the high-frequency transformer activates, letting current pass through the inductor L_o and the set of capacitors.

In the final phase, the energy continues to flow to the load as inductor L_o operates in CCM. The capacitor bank and freewheeling diode provide the necessary output energy to the load, while the current through inductor L_1 gradually decreases to zero as it discharges all its stored energy.

The improved Cuk converter demonstrates efficient power conversion, minimized voltage ripple, and high input power factor, making it well-suited for a wide range of power electronics applications.

2.2. Control strategy

A Proportional-Integral (PI) controller is employed in PSIM simulator to regulate both the output voltage and current of the proposed converter. To enhance dynamic performance, the controller is finally tuned to minimize steady-state error, enabling accurate power factor correction and reducing output voltage and current ripple. Unlike conventional control strategies that often exhibit limited adaptability to transient conditions, the optimized PI controller ensures robust regulation under varying load conditions. In voltage control mode, the system maintains a regulated 400V DC output, while in current control mode, it delivers a steady 3.5A charging current, adapting efficiently to load variations. This optimized control mechanism eliminates the need for additional PFC circuits, simplifying the design while maintaining a high power factor and ensuring effective charging operation.

The controller's performance is enhanced through careful selection of proportional gain and integral time constant value. This tuning enhances the controller's ability to respond efficiently to real-time voltage and current deviations, ensuring precise correction. As a result, the system maintains optimal stability and accuracy, effectively preserving the desired output voltage and current with minimal fluctuations.

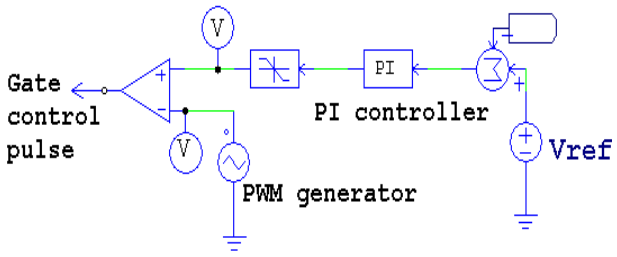

Fig. 2: PI Control Strategy for Closed-Loop Control.

The design of a PI controller for an AC-DC converter involves a structured methodology to efficiently regulate the output voltage and current through feedback loops, as illustrated in Figure 2. The voltage control loop constantly measures the output voltage and computes the error by comparing it to the desired set point, as defined in Equation 1.

$$e_v(t) = V_{ref} - V_{out}(t) \quad (1)$$

The PI controller utilizes the computed error to generate a corresponding control signal, $u_v(t)$ as shown in Equation 2.

$$u_v(t) = K_{pv} e_v(t) + K_{iv} \int e_v(t)\, dt \quad (2)$$

This signal is employed to adjust the duty cycle of the Pulse Width Modulation (PWM) signal or to alter the firing angle of the control switch to minimize voltage errors. In parallel, a current control loop operates during the converter operation, where the current error $e_i(t)$ defined in equation (3).

$$e_i(t) = I_{ref} - I_{out}(t) \quad (3)$$

The PI controller for the current loop generates a control signal $u_i(t)$ as per Equation (4).

$$u_i(t) = K_{pi} e_i(t) + K_{ii} \int e_i(t)\, dt \quad (4)$$

This allows adjustments to converter operation to prevent overcurrent conditions. To enhance the system's responsiveness and stability, a cascade control strategy is employed, where voltage control operates as the external loop and current control functions as the internal loop, allowing prioritized voltage regulation while maintaining rapid current control.
Integral windup is a common problem that can happen during changes in conditions. It can make the system unstable by causing errors in the integral part of the PI controller. To mitigate this, anti-windup techniques such as saturation limits on the control output are implemented. Tuning the proportional and integral gains is crucial for optimal performance. Methods such as Ziegler-Nichols provide systematic guidelines for establishing these gains based on system response characteristics. Validating the controller design through simulation in PSIM is an essential part of the development process. This simulation allows assessment of the system's performance under varying load conditions, enabling the observation of system behaviour and necessary adjustments for response time and stability.

3. Simulation

This study focuses on the simulation and evaluation of the simulated parameters for a Level-1 battery charger designed to deliver an output of 1.4 kW for electric vehicle battery charging. The charger operates using a standard domestic power source that can sufficiently charge electric vehicles under certain conditions. Specifically, the simulation models the converter to deliver a 400V, 3.5A DC output optimized for charging an electric car battery. The simulation model analyses charger performance, voltage regulation, and current stability during the charging process, ensuring that it meets the operational standards required for safe and effective battery charging. This study further explored the design considerations and technical specifications required to integrate such a charger into a typical home electrical infrastructure.
This simulation demonstrates an AC-DC converter design that delivers 1.4 kW power for electric vehicle battery charging. Many EVs use a 400V battery to power inverters and other equipment. This battery charger effectively charges the EV battery. Various standards govern battery chargers and establish crucial guidelines to ensure the safe and efficient operation of charging systems. These standards specify essential parameters such as the ripple voltage and ripple current. By defining acceptable limits for these parameters, the standards help minimize potential issues such as overheating and battery degradation. Ensuring compliance with these standards is vital for the charger to deliver stable and reliable power, which ultimately enhances the operation and longevity of a charged battery.
An EV battery can be charged using three primary methods: constant current, constant voltage, and trickle charging. CC charging provides a steady flow of electricity, making it efficient for quickly filling the battery with up to 80–85% of the battery SOC. In contrast, constant-voltage charging stabilizes the voltage, protecting the battery from overcharging as it approaches 98% of the battery's SOC capacity. Some advanced chargers combine the CC and CV methods and include trickle charging to optimize the charging process, ensuring that the battery is fully charged and maintained safely over time.

3.1. Converter charging control

The modified Cuk converter operates with a Li-ion battery connected as a load after PI tuning, involving dynamic interactions that facilitate efficient charging. Initially, the converter functions in CC charging mode, providing a steady current to the battery for rapid charging. This is essential in the early stages of accumulating energy.

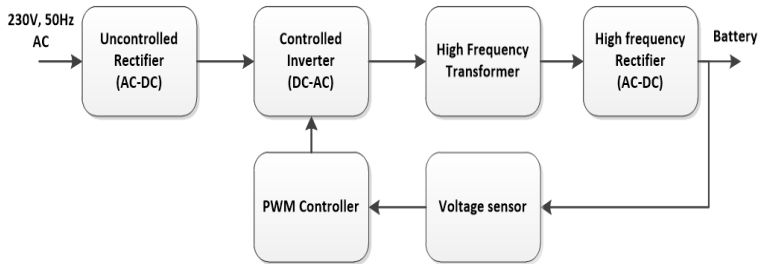

Fig. 3: Block Diagram of CC Control for Modified Cuk Converter Battery Charger.

As the battery approaches its target voltage, the system automatically transitions to the CV mode, maintaining a stable output voltage and allowing the charging current to gradually decrease as the battery is filled. This controlled approach helps prevent overcharging and prolongs battery life. Throughout the charging process, the converter continuously monitors the voltage and current and adjusts its operation to provide appropriate energy levels for efficient and safe battery charging.

During the battery charging process, the converter first operates in constant-current mode, allowing it to gain energy quickly and increase the battery pack voltage. Once the battery pack reaches 85% of its full voltage, the charging process transitions to constant-voltage mode. Figure 3 shows the circuit diagram of the Li-ion battery charger with closed-loop current control. The converter supplied a constant current of 3.5A for battery charging. In this simulation, the system sets the cell voltage to 3.2V, representing a fully discharged battery pack with a total voltage of 356V, and uses a PI control method to regulate battery charging effectively.

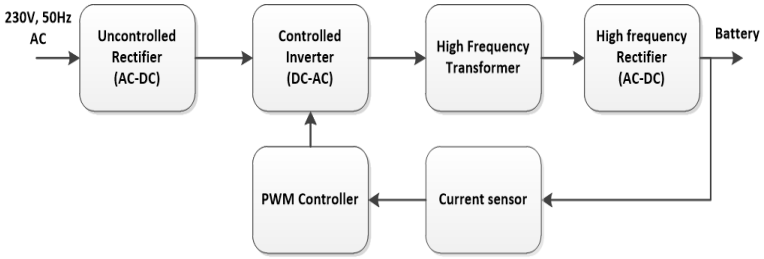

Fig. 4: Block Diagram of CV Control for Modified Cuk Converter Battery Charger.

Figure 4 shows the circuit diagram of the Li-ion battery charger for CV mode control. In this study, a Li-ion battery pack with a voltage rating of 400V connects to a converter for charging. In CV mode, the converter applies a constant voltage of 400V to the Li-ion battery, while the converter supplies a charging current of 3.5A.

During the CV charging phase, the battery gains energy, leading to a gradual reduction in the current flowing through the converter. Once the charging current decreases to 0.1% of the supply current, the system transitions into trickle charging mode, allowing the battery to store its full energy. This approach ensures efficient charging and enhances the overall lifespan of the batteries.

4. Results and discussion

The operation of the converter is evaluated in both CC and CV modes, with a Li-ion battery load. The converter efficiently supplies steady current during the initial charging phase, protecting the battery from overheating. The transition to CV mode is seamless, allowing for a consistent voltage output as the charging current decreases. This dual-mode operation optimizes charging effectiveness and enhances battery longevity.

4.1. CV mode performance

This section presents the simulation of the converter using PSIM, focusing on PI controller tuning to achieve effective voltage control. These simulations demonstrate that the converter operates in voltage control mode. The modified Cuk converter is operated in CV mode with a regulated 400V to charge the EV battery. The converter's parameters are then tested for performance in CV charging mode. Figures 10 to 14 display the converter waveforms during battery charging in CV control mode.

Figure 5 shows the battery-charging voltage and current waveforms for the constant-voltage control method. In this simulation, the battery cell voltage is assumed to be 3.5V, so the total battery pack voltage becomes 388.5V. The modified Cuk converter operates in CV mode. During this simulation of the battery charger, the converter maintains a constant 388.5V, and the battery draws a constant current of 3.5A.

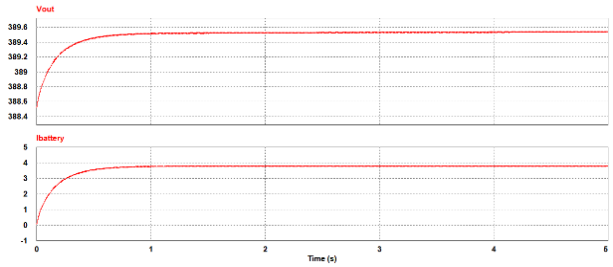

Fig. 5: Voltage and Current Waveforms of Li-Ion Battery During CV Charging Mode.

Figure 6 illustrates the detailed waveforms of the battery charging voltage and current during the constant-voltage mode operation. The waveforms demonstrate that both the voltage and current vary with less than 1% ripple. Consequently, the system minimizes heat generation and associated energy loss, allowing for efficient battery charging.

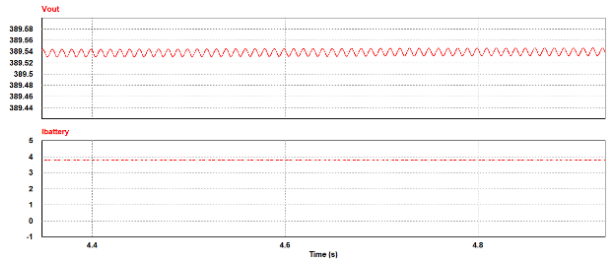

Fig. 6: Battery Charging Voltage and Current Waveforms Showing <1% Ripple During CV Mode.

In the CV charging mode, Figure 7 shows how the current flows through the intermediate capacitor and the filter. During each half-cycle of operation, the intermediate capacitor releases its stored energy, causing the current to drop to zero in both the capacitor and the inductor. This arrangement makes the input inductor work in DCM. This configuration is advantageous for achieving a high power factor.

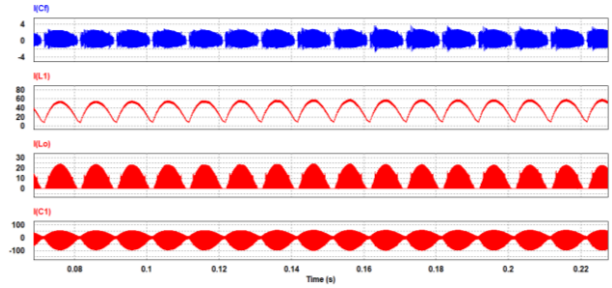

Fig. 7: Current Waveforms of Filter Component (C_f, L_1) Converter Capacitor (C_1) and Inductor (L_o) Using CV Mode Charging.

Figure 8 shows the source voltage and current waveforms for the input PF and diode bridge rectifier voltage. In CV mode of operation, the voltage across the bridge rectifier resembles a sine wave, peaking at 250V. This pulsating voltage can subsequently be converted to DC voltage using an LC filter. During constant-voltage operation, the source voltage and current yielded power factors of 0.96.

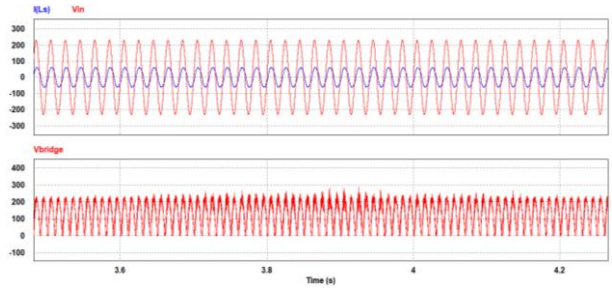

Fig. 8: Source Voltage, Current, and Input Power Factor (0.96) During CV Mode with Bridge Rectifier Output.

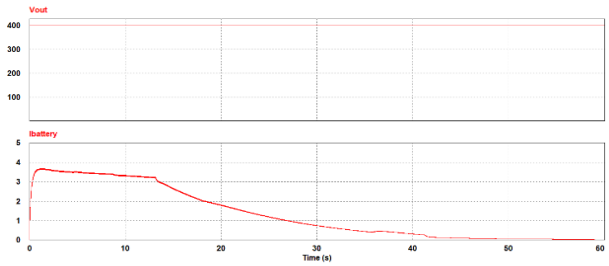

Fig. 9: Output Voltage and Declining Current Waveform During Final Stage of CV Charging Mode.

Figure 9 illustrates the battery charging current and voltage waveforms after the battery hits 400V. Once the battery voltage reaches its maximum set level, such as 400V, the CV charging mode begins. The supply voltage remained constant while the battery accumulated energy. As the battery charges and the voltage stabilizes, the battery gradually draws less current, indicating effective operation in the CV mode.

4.2. CC mode performance

Now, the simulations of the modified Cuk converter working in CC mode with a 400V Li-ion battery show that it delivers a steady charging current of 3.5A during the initial charging phase. This consistent current supply allows for rapid energy accumulation in the battery while preventing overheating and ensuring safe operation. Figures 10 to 14 show the converter waveforms for charging the battery in CC mode.

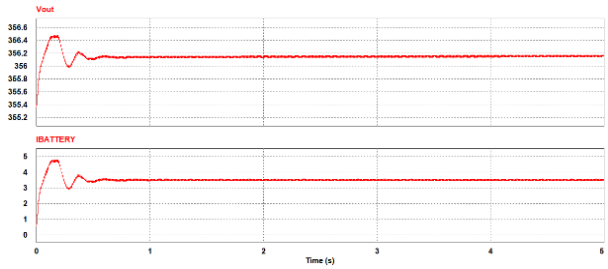

Fig. 10: Transient Response of Voltage and Current in Initial 5 Seconds of CC Mode With Fully Discharged Battery.

Figure 10 presents the charging current and voltage waveforms during battery charging, using the CC mode for a transient change in current while the battery is fully discharged. In this simulation, the voltage of a single lithium-ion cell is set to 3.2V, resulting in a total battery pack voltage of 356V in the fully discharged state. During the CC mode simulation, the initial battery voltage measures 356V, while the steady charging current is 3.5A.

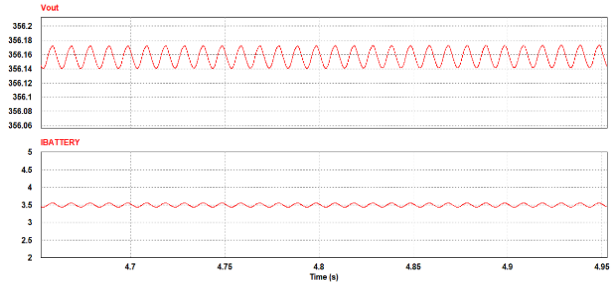

Fig. 11: Battery Charging Voltage and Current Waveforms During CC Mode.

Figure 11 illustrates an expanded view of the battery charging current and voltage during CC mode operation. The converter maintained a ripple value of less than 1% battery charging current. In addition, the system applies voltage to the battery pack, which exhibits a ripple below 1%. These low ripple values are beneficial to the health and lifespan of the batteries.

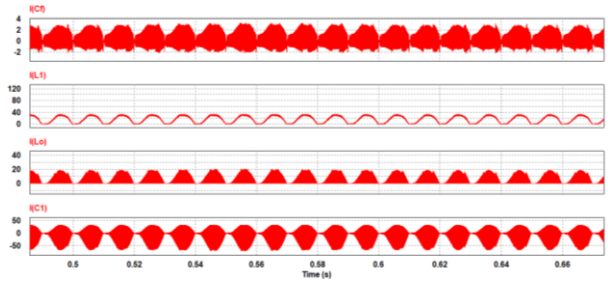

Fig. 12: Current Waveforms of Passive Components (C_f, L_1, C_1, L_o) During CC Charging Mode.

Figure 12 illustrates the currents of the filter capacitor, intermediate capacitor, filter inductor, and input inductor in CC charging mode. This figure demonstrates that during each half-cycle of operation, the capacitor releases its stored energy, resulting in the current decreasing to zero. As a result, the current flowing through the input inductor reaches zero at each half-cycle, causing the source inductor to operate in the DCM. This behavior is advantageous for achieving a favorable power factor (PF).
Figure 13 shows the source voltage and current waveforms for the input PF and diode bridge rectifier voltage. In the CC operation mode, the voltage across the bridge rectifier exhibited a sine-wave pattern, reaching a maximum value of 230V. An LC filter can convert this pulsating voltage into DC. Additionally, during the constant-current mode of operation, the source voltage and current achieved a power factor of 0.983.

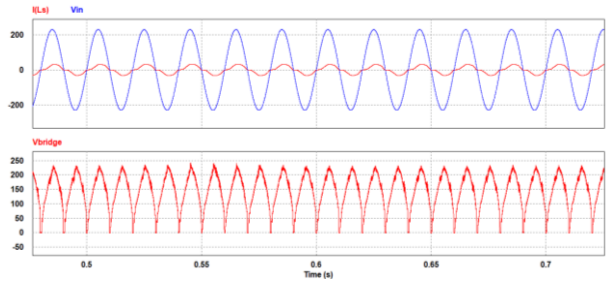

Fig. 13: Source Voltage, Current, and Input Power Factor (0.983) During CC Charging Mode with Bridge Rectifier Voltage.

During the CC charging mode, the battery charging current remains a constant 3.5A as the battery voltage begins to increase from its initial value. Figure 14 shows the battery voltage and current during this phase. The initial voltage of the fully discharged battery pack is 356V. As the battery charges in the CC mode, the voltage increases, whereas the charging current remains unchanged.

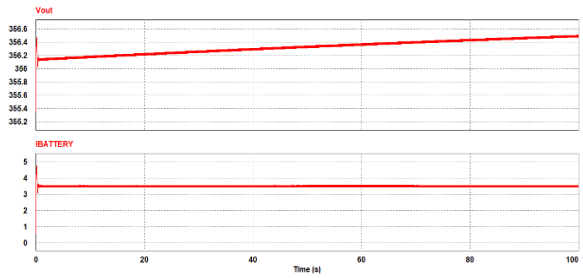

Fig. 14: Voltage Rise and Constant Current in CC Mode Starting from a Fully Discharged Battery.

This study assessed the operation of the converter in both CC and CV modes, with an EV battery as a load. The simulation of the modified Cuk converter efficiently provides a steady current during the initial charging phase, preventing battery overheating. The CV mode ensures a consistent voltage output as the charging current decreases. This dual-mode operation optimizes energy transfer quality and contributes to enhanced battery longevity.

4.3. Adaptability to varying conditions

There are many simulations run to fully test how the converter works with different input voltages (180V–280V) and loads. The primary objective is to assess the converter's ability to maintain stable operation under different operating scenarios. The modified Cuk converter effectively maintains stable voltage and current output across varying input conditions, ensuring consistent performance for EV charging applications. Unlike conventional converters, where power factor degrades significantly under fluctuating input voltages, this design maintains a high power factor between 0.87 and 0.97 across an input range of 180V–280V. The integration of DCM for the input inductor and CCM for the output inductor helps regulate power flow efficiently, minimizing the impact of voltage fluctuations.

The results show that the converter is reliable even when the input voltages and loads change. The output performance stays stable in both operational modes. This adaptability is essential for real-world applications where charging conditions can fluctuate frequently, ensuring reliable operation and maintaining the power factor across diverse scenarios.

This study explores the operation of a modified Cuk converter in both modes for battery charging, focusing on its performance under varying conditions. The proposed converter achieves high charging efficiency by maintaining a power factor above 0.98 and voltage and current ripple below 1%, outperforming conventional converter designs. In CC charging mode, the converter provides a stable 3.5A charging current, ensuring efficient energy transfer with minimal fluctuations. In CV charging mode, it maintains a steady 400V DC output, allowing the battery to charge safely while preventing overvoltage stress.

Table 2: Output Voltage Comparison Using Various Parameter Changes Using the Voltage Control Method

Supply Voltage (Vs)	Load	PF	Output Voltage (V)
230	Full Load	0.960	400
230	¾ load	0.960	400
200	Full Load	0.950	400
180	Full Load	0.910	400
250	Full Load	0.890	400
280	Full Load	0.870	400

The results obtained by the PI controller with the modified Cuk converter operating under the voltage control method are presented in Table 2. Additionally, the operation of the converter can be assessed by varying the input supply voltage. Notably, the output voltage remained stable despite input fluctuations. The table also illustrates how the power factor varies with changes in load and supply voltage. Specifically, a significant fluctuation in the input voltage, ranging from 180V to 280V, results in a PF variation from 0.97 to 0.87. Even at ¾ of the full load, the converter consistently maintains an output voltage of 400V.

Table 3: Output Current Comparison Using Various Parameter Changes Using the Current Control Method

Supply Voltage (Vs)	Load	Power Factor	Output Current (A)
230	Full Load	0.960	3.5
230	¾ load	0.970	3.5
200	Full Load	0.950	3.5
180	Full Load	0.940	3.5
250	Full Load	0.950	3.5
280	Full Load	0.960	3.5

Table 3 presents the results of testing the modified Cuk converter in the current control method. The converter is configured to use the PI controller. These changes enable the conversion to a variable constant current. Tests were conducted with variable input voltage, during which the output current remained steady at 3.5A. The converter is assessed under three-quarters of its full load, consistently delivering the same output current. Furthermore, when the supply voltage varies from 180V to 280V, the power factor varies from 0.94 to 0.97, respectively. Table 4 presents a comparison of the various parameters in the CC mode.

Table 4: Power Factor Comparison for Different State Battery Voltage Using CC Mode Charging

Cell Voltage (V)	Battery Voltage (V)	Power Factor	Output current (A)
3.2 (Discharged)	355.2	0.983	3.5
3.25	360.75	0.9827	3.5
3.3	366.3	0.9825	3.5
3.35	371.85	0.9823	3.5
3.4	377.4	0.982	3.5
3.45	382.95	0.9818	3.5
3.5	388.5	0.9815	3.5
3.55 (Charged)	394.05	0.9813	3.5

Table 5 presents a comparative analysis of various parameters in CV mode. This simulation utilized a lithium-ion battery to observe its voltage transition from a fully discharged state to a fully charged state. When fully discharged, the battery voltage measures 355.2V. Charging initiates at 356.2V in CV mode, where the input power factor is recorded at 0.966. As the battery gradually charges to 394V, the converter consistently outputs 395V, resulting in an input PF of 0.960. Importantly, the variation in the power factor throughout the constant-voltage charging process remained minimal, indicating a stable operation from the fully discharged to fully charged states.

Table 5: Power Factor Comparison for Different State Battery Voltage Using CV Mode Charging

Cell Voltage (V)	Battery Voltage (V)	Power Factor	Output Voltage (V)
3.2 (Discharged)	355.2	0.966	356.2
3.25	360.75	0.965	361.75
3.3	366.3	0.964	367.3
3.35	371.85	0.964	372.85
3.4	377.4	0.963	378.4
3.45	382.95	0.962	383.95
3.5	388.5	0.961	389.5
3.55 (Charged)	394.05	0.960	395.05

4.4. Comparative analysis of proposed converter

Table 6: Comparison of Different Converters with Modified Cuk Converter

Configuration attributes	Zhao et al. (2015)	Sabzali et al. (2011)		Proposed Modified Cuk converter
	Buck Boost	SEPIC	Cuk	
Polarity of Vout	-ve	+ve	-ve	+ve
No of switches	2	2	2	2
HFT	no	no	no	yes
Ultra-fast Diode	2	2	2	2
Conduction loss	5W	>5W	5W	3-5W
Output ripple	>5%	5%	3-5%	<2%
THD	20-30%	15-30%	20-30%	<10%
PF	0.95	0.96	0.965	0.98

Table 6 shows a comparison of different converters with a modified Cuk converter. The proposed modified Cuk converter demonstrates notable improvements over existing converters like those from Zhao et al. (2015) and Sabzali et al. (2011) [38-39]. The proposed modified Cuk converter offers significant advantages over conventional buck-boost, SEPIC, and traditional Cuk converters, particularly in terms of power factor, conduction losses, and total harmonic distortion (THD). The integration of a HFT and optimized PI control improves power quality by reducing THD to below 10%, compared to 20–30% in conventional designs.

In terms of efficiency, the proposed converter achieves lower conduction losses (3–5W), outperforming Buck-Boost and SEPIC converters, which typically exhibit >5W losses due to higher switching and conduction losses. The high power factor (0.98) further enhances its energy efficiency, surpassing Buck-Boost (0.95), SEPIC (0.96), and traditional Cuk converters (0.965). Additionally, the ripple voltage is maintained below 2%, which is a significant improvement over other converters that experience >5% ripple under variable load conditions.

These enhancements make the proposed converter a superior choice for EV battery charging, ensuring higher efficiency, lower power losses, and better power quality, ultimately extending battery lifespan and reducing energy consumption.

4.5. Hardware results

The proposed converter prototype has been designed for a 1.4 kW on-board battery charging application, as shown in Figure 15. A 50 kHz gate pulse is generated by an STM32G474VET6 microcontroller, featuring a 170 MHz ARM Cortex-M4 core, and it has been used in research for precise system control. Its advanced timers, high-resolution PWM channels, and built-in ADCs allow efficient real-time signal processing, making it perfect for generating accurate 50 kHz switching pulses. Additionally, it supports low-power operation and flexible communication interfaces for different power electronics applications.

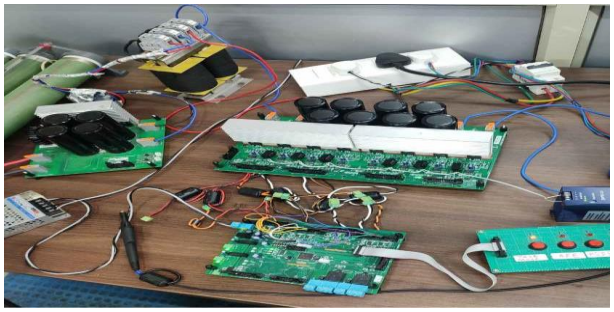

Fig. 15: Hardware Prototype of Proposed Converter for EV Charger.

In the system, the operation of the input inductor is at the normal frequency, while the operation of the charging side inductor is at 50 kHz. These inductors are constructed using ferrite core material. Polyester-type capacitors are selected for the application. To transform rectified DC to AC, the design incorporates the FQL40N50 Power MOSFET. For the input rectification, a 1N1184R diode is used, while the output rectification is handled by a (SiC)-based Schottky diode C3D08060A.

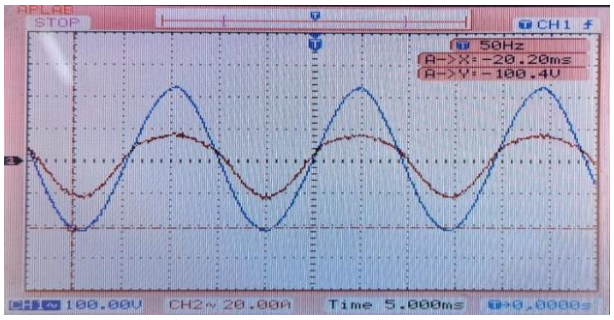

Fig. 16: Input Current and Voltage Waveform of Modified Cuk Converter Battery Charger.

Figure 16 presents the waveforms of the proposed charger, illustrating the input voltage and current under a rated battery load. The charger draws a sinusoidal input current of 16 A from the mains, with the source current following the sinusoidal envelope. This behavior reflects the charger's power quality (PQ) improvement capabilities. The measured input power factor (PF) is 0.975, and the total harmonic distortion (THD) of the current is 3.65%, both of which align with the IEC 61000-3-2 standard for enhanced power quality.

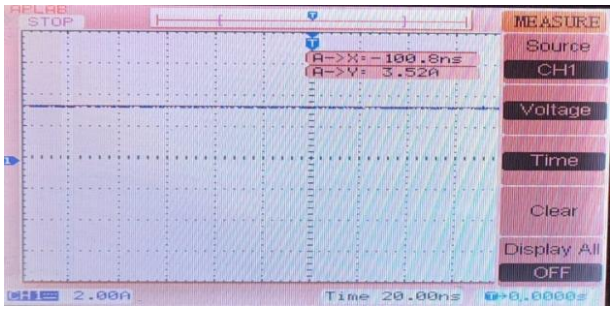

Fig. 17: Battery Charging Current of Modified Cuk Converter Battery Charger Showing 1.5% Ripple.

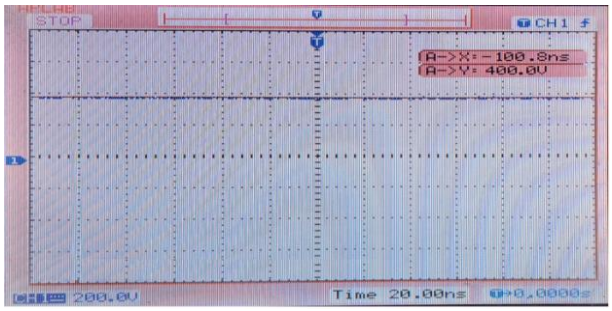

Fig. 18: Battery Charging Voltage of Modified Cuk Converter Battery Charger Showing 2% Ripple.

The battery charging current remains steady at 3.5A throughout the constant current (CC) charging mode. As shown in Figure 17, the ripple in the battery charging current is 1.5%. Figure 18 demonstrates that the modified Cuk converter maintains a constant 400V across its output, with a voltage ripple of only 2%. This minimal ripple helps minimize the risk of battery overheating.

The modified Cuk converter meets the IEC 61000-3-2 current harmonic distortion standard; however, commercial EV charging systems must follow international standards. SAE J1772, which controls North American EV charger connection and communication protocols, and ISO 15118, which defines vehicle-to-grid (V2G) communication standards for bidirectional energy transfer and plug-and-charge, are important. Secure digital communication, vehicle model compatibility, and better EMI shielding are required to meet these criteria. Implementing such protocols is difficult, particularly in tiny on-board charger designs, according to Santra et al. (2024). Integrating these standards involves electrical compliance and firmware-level flexibility, which may increase system cost and design overhead. As EV infrastructure globalizes, multi-standard compatibility will be necessary for widespread use of charger technologies like the modified Cuk converter.

5. Conclusion

The proposed modified Cuk converter demonstrates significant advancements over traditional topologies, including buck-boost, SEPIC, and standard Cuk converters. These improvements are especially evident in terms of ripple reduction, power quality, and overall performance in both CC and CV charging modes. Unlike conventional designs, which typically suffer from higher ripple (>5%) and lower power factors, the modified Cuk converter consistently maintains ripple below 2% and a power factor above 0.98, ensuring a stable and efficient charging process.

The converter's innovative design, which integrates a high-frequency transformer and optimized PI control, helps minimize switching losses and THD <10%, making it a highly reliable and energy-efficient solution for EV battery charging. Additionally, the converter's performance under varying input voltages (180V-280V) and different load conditions highlights its adaptability to fluctuating grid voltages, which is crucial in real-world charging environments. The power factor of the converter remains stable within the range of 0.87 to 0.97 despite the changes in input voltage, demonstrating the converter's ability to maintain efficient performance under a wide variety of input conditions.

The converter's ability to deliver low-ripple, high-quality power with minimal energy losses positions it as a superior choice for EV charging applications. Its ability and stable performance under both CC and CV modes ensure efficient energy transfer while reducing

stress on the battery, contributing to longer battery life and improved overall system efficiency. Furthermore, hardware testing confirmed the converter's power factor of 0.975 and the voltage and current ripple of less than 2%, aligning with the simulation results obtained using PSIM. The intrinsic low-ripple and high-power-factor characteristics may be beneficial for charging novel battery chemistries, such as solid-state batteries, which need accurate voltage and current control to ensure safety and efficiency. Jayalakshmi et al. (2024), the converter's high-frequency transformer facilitates galvanic separation, rendering it appropriate for bidirectional applications like vehicle-to-grid (V2G) systems.

Furthermore, scaling to high-power applications, such as Level-2 or Boost chargers, presents a challenge because the converter's topology may need to be redesigned to perfectly handle higher voltage and current ratings. Furthermore, the converter's thermal performance in harsh climatic circumstances, such as high ambient temperatures, warrants additional examination. Patel and Vyas (2024) identified similar challenges in their study of modified Cuk topologies, highlighting the need to choose components carefully and manage heat properly to ensure long-lasting reliability and efficiency. To address these constraints and improve the converter's applicability across a broader range of EV charging scenarios, further research should include temperature profiling, scalability analysis, and cost-performance optimization.

In conclusion. The proposed modified Cuk converter sets a new benchmark for EV charging technology. By combining exceptional ripple reduction, high power factor, and low ripple, it offers a practical and versatile solution that significantly enhances energy transfer quality, reduces energy losses, and contributes to the advancement of sustainable and efficient EV charging systems.

References

[1] Patil, D. and Agarwal, V., 2015. Compact on-board single-phase EV battery charger with novel low-frequency ripple compensator and optimum filter design. *IEEE Transactions on Vehicular Technology*, *65*(4), pp.1948-1956. https://doi.org/10.1109/TVT.2015.2424927.

[2] Kim, D. H., Kim, M. J., & Lee, B. K. (2016). An integrated battery charger with high power density and efficiency for electric vehicles. *IEEE Transactions on Power Electronics*, *32*(6), 4553-4565. https://doi.org/10.1109/TPEL.2016.2604404.

[3] Sujitha, N. and Krithiga, S., 2017. RES based EV battery charging system: A review. *Renewable and Sustainable Energy Reviews*, *75*, pp.978-988. https://doi.org/10.1016/j.rser.2016.11.078.

[4] Lu, J., Bai, K., Taylor, A.R., Liu, G., Brown, A., Johnson, P.M. and McAmmond, M., 2017. A modular-designed three-phase high-efficiency high-power-density EV battery charger using dual/triple-phase-shift control. *IEEE Transactions on Power Electronics*, *33*(9), pp.8091-8100. https://doi.org/10.1109/TPEL.2017.2769661.

[5] Nguyen, H.V., To, D.D. and Lee, D.C., 2018. On-board battery chargers for plug-in electric vehicles with dual functional circuit for low-voltage battery charging and active power decoupling. *IEEE Access*, *6*, pp.70212-70222. https://doi.org/10.1109/ACCESS.2018.2876645.

[6] Kushwaha, R. and Singh, B., 2018, September. An improved battery charger for electric vehicle with high power factor. In *2018 IEEE Industry Applications Society Annual Meeting (IAS)* (pp. 1-8). IEEE https://doi.org/10.1109/IAS.2018.8544585.

[7] Yilmaz, U., Turksoy, O. and Teke, A., 2020. Improving a battery charger architecture for electric vehicles with photovoltaic system. *International Journal of Energy Research*, *44*(6), pp.4376-4394. https://doi.org/10.1002/er.5211.

[8] Lai, C. P. Y., Law, K. H., & Lim, K. H. (2020, October). Photo-voltaic Powered Electric Vehicle Fast Charger. In *IOP Conference Series: Materials Science and Engineering* (Vol. 943, No. 1, p. 012014). IOP Publishing. https://doi.org/10.1088/1757-899X/943/1/012014.

[9] Tiwary, A. and Singh, M., 2020. A modified PFC rectifier based EV charger employing CC/CV mode of charging. *IFAC-Papers On Line*, *53*(2), pp.13551-13556. https://doi.org/10.1016/j.ifacol.2020.12.799.

[10] Kushwaha, R. and Singh, B., 2021. A high-power quality battery charger for light electric vehicle using switched inductor PFC converter. *IET Power electronics*, *14*(1), pp.120-131. https://doi.org/10.1049/pel2.12016.

[11] TO Berliner, M. D., Jiang, B., Cogswell, D. A., Bazant, M. Z., & Braatz, R. D. (2022). Novel operating modes for the charging of lithium-ion batteries. *Journal of The Electrochemical Society*, *169*(10), 100546. https://doi.org/10.1149/1945-7111/ac9a80.

[12] Patel, N., Lopes, L.A., Rathore, A. and Khadkikar, V., 2023. A Soft-Switched Single-Stage Single-Phase PFC Converter for Bidirectional Plug-In EV Charger. *IEEE Transactions on Industry Applications*, *59*(4), pp.5123-5135. https://doi.org/10.1109/APEC43580.2023.10131495.

[13] Sisir, Singh, S. and Bharath, 2023, June. DSP Based Inbuilt Active PFC Battery Charger. In *International Conference on Intelligent Manufacturing and Energy Sustainability* (pp. 247-256). Singapore: Springer Nature Singapore. https://doi.org/10.1007/978-981-99-6774-2_23.

[14] Kushwaha, R. and Singh, B., 2019. A modified luo converter-based electric vehicle battery charger with power quality improvement. *IEEE Transactions on Transportation Electrification*, *5*(4), pp.1087-1096. https://doi.org/10.1109/TTE.2019.2952089.

[15] Jagadeesh, I. and Indragandhi, V., 2019, October. Review and comparative analysis on dc-dc converters used in electric vehicle applications. In *IOP Conference Series: Materials Science and Engineering* (Vol. 623, No. 1, p. 012005). IOP Publishing. https://doi.org/10.1088/1757-899X/623/1/012005.

[16] Kushwaha, R. and Singh, B., 2020. Interleaved landsman converter fed EV battery charger with power factor correction. *IEEE Transactions on Industry Applications*, *56*(4), pp.4179-4192. https://doi.org/10.1109/TIA.2020.2988174.

[17] Dixit, A., Pande, K., Gangavarapu, S. and Rathore, A.K., 2020. DCM-based bridgeless PFC converter for EV charging application. *IEEE Journal of Emerging and Selected Topics in Industrial Electronics*, *1*(1), pp.57-66. https://doi.org/10.1109/JESTIE.2020.2999595.

[18] Choi, S.W., Oh, S.T., Kim, M.W., Lee, I.O. and Lee, J.Y., 2020. Interleaved isolated single-phase PFC converter module for three-phase EV charger. *IEEE Transactions on Vehicular Technology*, 69(5), pp.4957-4967. https://doi.org/10.1109/TVT.2020.2980878.

[19] Pandey, R. and Singh, B., 2021. A power factor corrected resonant EV charger using reduced sensor based bridgeless boost PFC converter. *IEEE Transactions on Industry Applications*, *57*(6), pp.6465-6474. https://doi.org/10.1109/TIA.2021.3106616.

[20] Papamanolis, P., Bortis, D., Krismer, F., Menzi, D. and Kolar, J.W., 2021. New EV battery charger PFC rectifier front-end allowing full power delivery in 3-phase and 1-phase operation. *Electronics*, *10*(17), p.2069. https://doi.org/10.3390/electronics10172069.

[21] Devia-Narvaez, D.F., Devia-Narvaez, D.M. and Castillo Rodríguez, N.J., 2021, October. A new opto-isolator circuit topology for a three-phase alternating current/direct current converter. In *Journal of Physics: Conference Series* (Vol. 2046, No. 1, p. 012022). IOP Publishing. https://doi.org/10.1088/1742-6596/2046/1/012022.

[22] Kumar, G.N. and Verma, A.K., 2021, December. A two-stage interleaved bridgeless PFC based on-board charger for 48V ev applications. In *2021 IEEE 2nd International Conference on Smart Technologies for Power, Energy and Control (STPEC)* (pp. 1-5). IEEE. https://doi.org/10.1109/STPEC52385.2021.9718757.

[23] Dutta, S., Gangavarapu, S., Rathore, A.K., Singh, R.K., Mishra, S.K. and Khadkikar, V., 2022. Novel single-phase Cuk-derived bridgeless PFC converter for on-board EV charger with reduced number of components. *IEEE Transactions on Industry Applications*, *58*(3), pp.3999-4010. https://doi.org/10.1109/TIA.2022.3148969.

[24] Jain, A., Gupta, K.K., Jain, S.K. and Bhatnagar, P., 2022. A bidirectional five-level buck PFC rectifier with wide output range for EV charging application. *IEEE Transactions on Power Electronics*, *37*(11), pp.13439-13455. https://doi.org/10.1109/TPEL.2022.3185239.

[25] Chaithanya, S. and Sindhu, M.R., 2022, May. A PFC based on-board battery charger using isolated full-bridge DC-DC converter for electric vehicle application. In *2022 IEEE IAS Global Conference on Emerging Technologies (GlobConET)* (pp. 581-586). IEEE. https://doi.org/10.1109/GlobConET53749.2022.9872512.

[26] Tiwari, A.K., Sahu, L.K. and Barwar, M.K., 2023. Single-phase five-level PFC rectifier-based isolated electric vehicle battery charger. *Electrical Engineering*, *105*(4), pp.2137-2150. https://doi.org/10.1007/s00202-023-01799-2.

[27] Kumar, G.N. and Verma, A.K., 2023. A single-phase interleaved buck-boost pfc based on-board ev charger. *IEEE Transactions on Industry Applications*. https://doi.org/10.1109/TIA.2023.3302269.
[28] Patel, P. B., & Vyas, S. R. (2024). Improving DC power supply performance: insights into Cuk and modified Cuk converters' stability and power factor. *Engineering Research Express*, *6*(4), 045334. https://doi.org/10.1088/2631-8695/ad8d31.
[29] Bag, K., Mundra, M. P., Sadashiv, P. S., Sudarshan, B. S., & Arunkumar, G. (2024). Modeling, design and validation of DC-DC landsman converter for low-power electric vehicle battery charging applications. *Engineering Research Express*, *6*(3), 035306. https://doi.org/10.1088/2631-8695/ad5e35.
[30] Jayalakshmi, N. S., Sathe, M., Pandey, A. K., & Jadoun, V. K. (2024). Investigating the potential advancements for electric vehicle charging technologies through various converters topology. *Engineering Research Express*, *6*(4), 042302. https://doi.org/10.1088/2631-8695/ad8064.
[31] Chang, C., He, L., Bian, B. and Han, X., 2019. Design of a highly accuracy PSR CC/CV AC–DC converter based on a cable compensation scheme without an external capacitor. *IEEE Transactions on Power Electronics*, *34*(10), pp.9552-9561. https://doi.org/10.1109/TPEL.2019.2893737.
[32] Stübler, T., Lahyani, A. and Zayoud, A.A., 2020. Lithium-ion battery modeling using CC–CV and impedance spectroscopy characterizations. *SN Applied Sciences*, *2*(5), p.817. https://doi.org/10.1007/s42452-020-2675-6.
[33] Li, H., Zhang, X., Peng, J., He, J., Huang, Z. and Wang, J., 2020. Cooperative CC–CV charging of supercapacitors using multicharger systems. *IEEE Transactions on Industrial Electronics*, *67*(12), pp.10497-10508. https://doi.org/10.1109/TIE.2019.2962485.
[34] Liu, H., Naqvi, I.H., Li, F., Liu, C., Shafiei, N., Li, Y. and Pecht, M., 2020. An analytical model for the CC-CV charge of Li-ion batteries with application to degradation analysis. *Journal of Energy Storage*, *29*, p.101342. https://doi.org/10.1016/j.est.2020.101342.
[35] Nguyen, H.T., Alsawalhi, J.Y., Al Hosani, K., Al-Sumaiti, A.S., Al Jaafari, K.A., Byon, Y.J. and El Moursi, M.S., 2021. Review map of comparative designs for wireless high-power transfer systems in EV applications: Maximum efficiency, ZPA, and CC/CV modes at fixed resonance frequency independent from coupling coefficient. *IEEE Transactions on Power Electronics*, *37*(4), pp.4857-4876. https://doi.org/10.1109/TPEL.2021.3124293.
[36] De, A.K. and Dey, S., 2021. Establishment of transition point in operating mode for Constant Current Constant Voltage (CC-CV) charging of Li-ion batteries. *World Journal of Advanced Engineering Technology and Sciences*, *3*(1), pp.072-083. https://doi.org/10.30574/wjaets.2021.3.1.0053.
[37] He, L., Wang, X. and Lee, C.K., 2023. A study and implementation of inductive power transfer system using hybrid control strategy for CC-CV battery charging. *Sustainability*, *15*(4), p.3606. https://doi.org/10.3390/su15043606.
[38] Zhao, B., Abramovitz, A., & Smedley, K. (2015). Family of bridgeless buck-boost PFC rectifiers. *IEEE Transactions on Power Electronics*, *30*(12), 6524-6527. https://doi.org/10.1109/TPEL.2015.2445779.
[39] Sabzali, A. J., Ismail, E. H., Al-Saffar, M. A., & Fardoun, A. A. (2011). New bridgeless DCM Sepic and Cuk PFC rectifiers with low conduction and switching losses. *IEEE Transactions on Industry Applications*, *47*(2), 873-881. https://doi.org/10.1109/TIA.2010.2102996.